

AXISYMMETRIC FREE CONVECTION BOUNDARY-LAYER FLOW PAST SLENDER BODIES

H. K. KUIKEN *

Department of Mathematics, Technological University Delft, The Netherlands

(Received 5 December 1966 and in revised form 12 January 1968)

Abstract—Radial curvature effects on axisymmetric free convection boundary-layer flow are investigated for vertical cylinders and cones for some special non-uniform temperature differences between the surface and the ambient fluid. The solution is given as a power series expansion, the first term being equal to the solution to be found when no transverse curvature is involved. For a variety of Prandtl numbers numerical integrations have been carried out. An interesting application is the determination of the surface temperature of a free-convection-cooled cylinder with constant heat flux through the surface. For the Prandtl numbers considered, it turns out that the same heat flux induces a lower surface temperature on a cylinder than on a flat plate.

NOMENCLATURE

c , dimensionless number;
 c_1 , dimensionless number;
 c_p , specific heat at constant pressure [J/kg°K];
 f , dependent variable representing the stream function;
 f_m , expansion coefficient;
 g , acceleration due to gravity [m/s²];
 Gr_x , local Grashof number;
 h , part of the surface temperature;
 k , thermal conductivity [J/ms°K];
 l , some length (see definition \bar{x}) [m];
 m , exponent in surface temperature;
 N , constant having dimension of temperature [°K];
 Nu_x , local Nusselt number;
 q , heat flux [J/m² s];
 r , distance to the axis of symmetry [m];
 r_0 , radius of cylinder [m];
 T , temperature [°K];
 T_w , temperature of the surface of the body [°K];

T_∞ , ambient temperature [°K];
 u , velocity component in x -direction [m/s];
 v , velocity component in y -direction [m/s];
 x , longitudinal coordinate [m];
 \bar{x} , dimensionless longitudinal coordinate, (x/l);
 y , coordinate in y -direction [m].

Greek symbols

β , coefficient of thermal expansion [°K];
 η , dimensionless coordinate;
 $\bar{\eta}$, Sparrow–Gregg similarity variable;
 η_{is} , similarity variable for isothermal flat plate;
 ϕ , angle between axis and tangent plane to the surface;
 ψ , stream function [m³/s];
 ν , kinematic viscosity [m²/s];
 ρ , density of the fluid [kg/m³];
 σ , Prandtl number;
 θ , dimensionless temperature;
 θ_m , expansion coefficient;
 ξ , expansion variable.

* Present address: Unsteady Aerodynamics Laboratory, National Research Council, Ottawa, Ontario, Canada.

Subscripts

∞ , ambient conditions;

- n , expansion integer;
 w , wall conditions;
 A prime denotes differentiation with respect to η .

1. INTRODUCTION

THE INFLUENCE of radial curvature on axisymmetric boundary-layer flow has been investigated in many papers and in great detail. If thermal effects are taken into account, however, the bulk of these papers deals with forced convection. Examples are the references [1-5]. Only a few investigations concerning this matter have been performed in the field of free convection. Sparrow and Gregg [6] gave a series solution for free convection boundary-layer flow along a vertical cylinder with constant surface temperature. This problem has also been looked into by Hama and Christiaens [7]. Millsaps and Pohlhausen [8] and Yang [9] showed the possibility of reducing the governing partial differential equations to ordinary ones in the case of a vertical cylinder with a surface temperature varying linearly with the distance from the leading edge. Other papers investigating free convection in axisymmetric flow did not take the transverse curvature of the surface into account [10-13].

In this paper, the influence of a small radius of curvature (comparable with the thickness of the boundary layer) on laminar free convection boundary-layer flow will be treated more extensively than has been done to date. To this end the two most simple bodies of small radii of curvature, i.e. (1) the thin cylinder, (2) the slender cone, are singled out. The surface temperatures to be allowed belong to a certain class of non-linear functions of the longitudinal coordinate x .

It is not possible here, as in many other boundary-layer problems, to transform the governing differential equations by using a similarity variable only. An expansion variable has to be introduced as well. The solution will be given as a power expansion in this variable, the coefficients being functions of a variable to

be called "similar" for simplicity, although this is not true in the proper sense of the word.

The first term of this expansion is, as expected, the same as the solution one will have when no transverse curvature is involved. So, in view of the wall temperatures allowed, the flat plate solution given by Sparrow and Gregg [14] and by Finston [15] constitutes the first term of the present solution for the cylinder. In the case of the slender cone, the solution of Hering and Grosh [13] will occur as the first term of the series. In dealing with flow around cylinders and cones, the present approach is inspired by that of [14] and [13] respectively.

Equations and boundary conditions

In carrying out the analysis in this paper, the condition be imposed that the temperature of the body everywhere exceeds that of the ambient fluid. As a consequence the flow will be in upward direction. In other papers it has already been argued that the reverse case is mathematically the same [6, 14]. Furthermore the assumption is maintained that all fluid properties be constant with the exception of those causing the effect of buoyancy. This means the retention of the effect of volumetric expansion in the momentum equation, but the dropping of it in the equation of continuity. Ostrach deals thoroughly with these assumptions and their limitations [16].

As is well known, the free convection boundary-layer flow is governed by a set of three partial differential equations. For axisymmetric flow these are:

1. The equation of continuity

$$\frac{\partial}{\partial x}(ru) + \frac{\partial}{\partial y}(rv) = 0, \quad (1)$$

2. The momentum equation

$$u \frac{\partial u}{\partial x} + v \frac{\partial u}{\partial y} = \frac{\nu}{r} \frac{\partial}{\partial y} \left(r \frac{\partial u}{\partial y} \right) + g\beta(T - T_\infty) \cos \phi, \quad (2)$$

3. The energy equation

$$u \frac{\partial T}{\partial x} + v \frac{\partial T}{\partial y} = \frac{k}{\rho c_p} \frac{1}{r} \frac{\partial}{\partial y} \left(r \frac{\partial T}{\partial y} \right). \quad (3)$$

The usual way of solving the equation of continuity is the introduction of the stream function ψ with

$$u = \frac{1}{r} \frac{\partial \psi}{\partial y}, \quad v = -\frac{1}{r} \frac{\partial \psi}{\partial x}. \quad (4)$$

The integration of the remaining equations (2) and (3) for a general slender body of revolution seems to be very difficult. To support this statement, reference may be made to a paper of Braun, Ostrach and Heighway [12] who tried to specify bodies allowing for similarity solutions in free convection boundary-layer flow. Although they use the operator

$$\frac{\partial^2}{\partial y^2}$$

instead of

$$\frac{1}{r} \frac{\partial}{\partial y} \left(r \frac{\partial}{\partial y} \right)$$

in equations (2) and (3) as a simplification, their work is of considerable complexity.

In other fields of boundary-layer flow transformations for axisymmetric flow around a general slender body have been given. Probstein and Elliot [3] and Wei [5] give a general transformation for forced convection flow along thin axisymmetric bodies. In their analyses it turns out however, that a ready solution can only be obtained for some specific classes of bodies. The reason for this is that the transformed equations contain complicated coefficients, which are functions of the original coordinates. Of the specific class of bodies for which these coefficients are simple, only the cylinder and cone are of practical importance. For reasons of pragmatism we therefore investigate these bodies directly.

It may be remembered that the phenomenon just discussed also occurs in the transformation

of Görtler, which leaves the Görtler principal function in the transformed equation. This function has to satisfy certain conditions to allow a solution in series [17].

As far as the dynamic part of the problem is concerned, three boundary conditions have to be introduced: $u = v = 0$ at the surface of the body and $u = 0$ at the outer edge of the boundary layer ($y \rightarrow \infty$). The temperature has to satisfy two conditions. Obviously one of these is $T \rightarrow T_\infty$ as $y \rightarrow \infty$. The condition at the surface of the body will be given as:

$$T_w = T_\infty + N \bar{x}^m h(x). \quad (5)$$

Here $h(x)$ is a function of the variable $\xi(x)$ to be defined in the next section. In view of the method of solution developed in this paper $h(x)$ has to be a series expansion in ξ of the following kind

$$h(x) = 1 + a_1 \xi + a_2 \xi^2 + \dots \quad (6)$$

2. CYLINDER

(a) Analysis

If $y = r - r_0$ and $\phi = 0$, the equations (1–3) govern free convection past a vertical circular cylinder (Fig. 1). Instead of the coordinates x and r , two other coordinates will be used

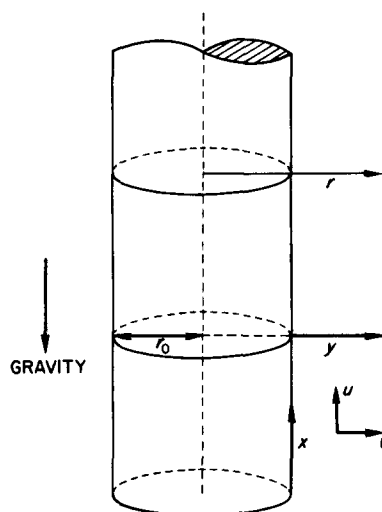


FIG. 1. Geometrical configuration for flow past cylinder.

which are more suitable to obtain a solution. Let these coordinates be:

$$\xi = \frac{2l}{cr_0} \bar{x}^{\frac{1-m}{4}}, \quad (7)$$

$$\eta = \frac{r^2 - r_0^2}{r_0^2 \xi}, \quad (8)$$

where c is given by

$$c = \left(\frac{g\beta N l^3}{4\nu^2} \right)^{\frac{1}{4}}. \quad (9)$$

Two reasons can be given to justify the choice of η in equation (8). First, it is seen that the boundary conditions at the surface of the cylinder are satisfied for $\eta = 0$, while those at the outer edge of the boundary layer correspond with $\eta \rightarrow \infty$ ($r \rightarrow \infty$). This obviously is very convenient from a mathematical point of view. A second, and more important reason follows from the asymptotic behaviour of η for $r_0 \rightarrow \infty$.

$$\begin{aligned} \lim_{r_0 \rightarrow \infty} \eta &= \lim_{r_0 \rightarrow \infty} \frac{c}{2r_0 l} \{(r_0 + y)^2 - r_0^2\} \bar{x}^{\frac{m-1}{4}} \\ &= \frac{cy}{l} \bar{x}^{\frac{m-1}{4}} = \bar{\eta}. \end{aligned} \quad (10)$$

Sparrow and Gregg [14] have proved that free convection past a non-isothermal vertical flat plate having the temperature

$$T_w = T_\infty + N\bar{x}^m \quad (11)$$

can be described by using the similarity variable

$$\bar{\eta} = \frac{cy}{l} \bar{x}^{\frac{m-1}{4}} \quad (12)$$

Because of this, the asymptotic behaviour of η as given in equation (10) is actually required since on having r_0 approach infinity for a fixed value of x and for a fixed wall-temperature the flow along a vertical cylinder should more and more resemble that along a flat plate. As $\lim_{r_0 \rightarrow \infty} \xi = 0$, the wall temperatures presented in equation (5) approach the temperatures (11) considered by Sparrow and Gregg.

The reason for introducing the second independent variable ξ is closely related to the fact that a boundary layer of free convection becomes thinner as the temperature difference between the wall and the ambient fluid grows. This can be shown directly with the simple similarity variable applying to the isothermal flat plate

$$\bar{\eta}_i = y \left(\frac{g\beta(T_w - T_\infty)}{4\nu^2 x} \right)^{\frac{1}{4}}. \quad (13)$$

If the temperature-difference $T_w - T_\infty$ becomes larger, the outer edge of the boundary layer is reached for a smaller value of y . This conclusion is justified, since numerical calculations show that the outer edge of the boundary layer is reached with a high degree of accuracy for, say $\bar{\eta}_i = 10$. An investigation of the more general Sparrow-Gregg wall-temperatures [11] reveals the same feature of the free convection boundary layer.

For $m > 0$ the temperature difference $T_w - T_\infty$ grows in the downstream direction. On inspection of equation (12) it is seen, however, that only for $m > 1$ the boundary layer becomes thinner if x grows, i.e. in the direction of the growing temperature-differences. As an explanation one naturally can say that a boundary layer always tends to become thicker in downstream direction. The rate at which $T_w - T_\infty$ has to grow must be sufficiently large to curb this tendency. Apparently for $m > 1$ this aim is achieved. Accordingly, it may be expected that for $x \rightarrow \infty$ and $m > 1$ the free convection boundary layer along a vertical cylinder will tend to that of Sparrow and Gregg, established for the flat plate. This conclusion is based upon the fact that the influence of radial curvature disappears as the thickness of the boundary layer approaches zero. For $m < 1$ the situation is just reverse. The boundary-layer thickness is zero at the leading edge and grows in downstream direction. Inspection of equation (7) shows that ξ tends to zero if x approaches the region where the solution for the flat plate is valid. As a regular perturbation of the flat plate

solution will supply information about the influence of radial curvature, it is clear that ξ can be used as a perturbation variable. For $m > 1$ ξ vanishes in downstream direction, while for $m < 1$, ξ is equal to zero at the leading edge. For $m = 1$, ξ is a constant which suggests that a similarity solution can be found. Such a solution has been presented already by Millsaps and Pohlhausen [8].

The stream function ψ and the temperature T are now expressed in ξ and η by introduction of dimensionless functions

$$\psi = 4\nu r_0 c \bar{x}^{\frac{m+3}{4}} f(\xi, \eta), \quad (14)$$

$$T = T_\infty + N \bar{x}^m \theta(\xi, \eta). \quad (15)$$

Here the correspondence with the work of Sparrow and Gregg is complete, apart from a slight modification of the coefficient in equation (14) and the fact that f and θ depend on ξ also. The substitution of (7, 8, 14, 15) in the equations (2) and (3) is an awkward and lengthy procedure, of which no details will be given here. The result is

$$\begin{aligned} & \frac{\partial^3 f}{\partial \eta^3} + (m+3) f \frac{\partial^2 f}{\partial \eta^2} - 2(m+1) \left(\frac{\partial f}{\partial \eta} \right)^2 + \theta \\ & + \xi \left[\frac{\partial^2 f}{\partial \eta^2} + \eta \frac{\partial^3 f}{\partial \eta^3} + (m-1) \right. \\ & \quad \times \left. \left(\frac{\partial f}{\partial \eta} \frac{\partial^2 f}{\partial \eta \partial \xi} - \frac{\partial f}{\partial \xi} \frac{\partial^2 f}{\partial \eta^2} \right) \right] = 0, \end{aligned} \quad (16)$$

$$\begin{aligned} & \frac{1}{\sigma} \frac{\partial^2 \theta}{\partial \eta^2} + (m+3) f \frac{\partial \theta}{\partial \eta} - 4m \theta \frac{\partial f}{\partial \eta} \\ & + \xi \left[\frac{1}{\sigma} \left(\frac{\partial \theta}{\partial \eta} + \eta \frac{\partial^2 \theta}{\partial \eta^2} \right) + (m-1) \right. \\ & \quad \times \left. \left(\frac{\partial f}{\partial \eta} \frac{\partial \theta}{\partial \xi} - \frac{\partial f}{\partial \xi} \frac{\partial \theta}{\partial \eta} \right) \right] = 0, \end{aligned} \quad (17)$$

where $\sigma = (\nu \rho c_p / k)$ is the Prandtl number. It is easy to derive that the boundary conditions to be imposed on f and θ are

$$f = \frac{\partial f}{\partial \eta} = 0, \quad \theta = h(x)$$

$$= 1 + \sum_{n=0}^{\infty} a_n \xi^n \quad \text{at } \eta = 0,$$

$$\frac{\partial f}{\partial \eta} = \theta \rightarrow 0 \quad \text{as } \eta \rightarrow \infty. \quad (18)$$

At first sight the transformation did not lead to any simplifications, but a more careful observation of the system of equations (16) and (17) with the conditions (18) shows that it is suited to perturbation techniques. It may be expected that the equations can be solved through substitution of

$$f(\xi, \eta) = \sum_{n=0}^{\infty} f_n(\eta) \xi^n, \quad (19)$$

$$\theta(\xi, \eta) = \sum_{n=0}^{\infty} \theta_n(\eta) \xi^n, \quad (20)$$

in the equations (16) and (17). In fact on writing ξ as

$$\xi = 2^{\frac{1}{2}} \left(\frac{h}{Gr_x} \right)^{\frac{1}{4}} \frac{x}{r_0} \quad (21)$$

where

$$Gr_x = \frac{g \beta (T_w - T_\infty) x^3}{\nu^2} \quad (22)$$

is the local Grashof number, it is seen that ξ tends to zero as $r_0 \rightarrow \infty$ for x constant. In this case the contribution of the terms with $f_n(\eta)$ and $\theta_n(\eta)$ ($n > 0$) to $f(\xi, \eta)$ and $\theta(\xi, \eta)$ vanishes, yielding

$$\lim_{\substack{r_0 \rightarrow \infty \\ x \text{ const.}}} f(\xi, \eta) = f_0(\bar{\eta}), \quad \lim_{\substack{r_0 \rightarrow \infty \\ x \text{ const.}}} \theta(\xi, \eta) = \theta_0(\bar{\eta}). \quad (23)$$

Insertion of (19) and (20) in (16) and (17) renders as zeroth perturbation, the set of ordinary differential equations found by Sparrow and Gregg; this describes free convection along a vertical flat plate engendered by the wall temperature of equation (5) with $h = 1$

$$\begin{aligned} & f_0''' + (m+3) f_0 f_0'' - 2(m+1) (f_0')^2 \\ & + \theta_0 = 0, \quad \frac{1}{\sigma} \theta_0'' + (m+3) f_0 \theta_0' \\ & - 4m f_0' \theta_0 = 0. \end{aligned} \quad (24)$$

Furthermore it should be noted that the expansion variable ξ is proportional to the inverse of the fourth root of the Grashof number. If Gr_x grows due to variations of g , β or N , the influence of radial curvature decreases. As x occurs in ξ , outside Gr_x , a variation of this variable can have different effects. However, these have been discussed already. In view of the fact that the function f_n depends upon the Prandtl number σ , the effect of viscosity ν on the influence of radial curvature is twofold. An example to be expounded in a later section shows that the resultant effect is that the influence of the transverse curvature is reduced as ν becomes smaller.

The functions of the first and higher perturbations satisfy systems of two linear non-homogeneous differential equations. The non-homogeneous parts contain the functions of the previous perturbations. Concerning this, reference may be made to a paper of Sparrow and Gregg [6] where these authors elaborate the case of a cylinder with a constant wall temperature.

(b) Heat transfer

The local heat transfer from the surface of the cylinder to the fluid has to be derived from Fourier's law

$$q = -k \left[\frac{\partial T}{\partial y} \right]_{y=0} \quad (25)$$

For the present problem this gives

$$q = -\frac{kcN}{l} \bar{x}^{\frac{5m-1}{4}} \left[\frac{\partial \theta}{\partial \eta} \right]_{\eta=0} \quad (26)$$

More generally, the local heat flux is represented by the dimensionless quantity

$$\frac{Nu_x}{Gr_x^{\frac{1}{4}}} = -(4h^5)^{-\frac{1}{4}} \sum_{n=0}^{\infty} \theta'_n(0) \xi^n. \quad (27)$$

where Nu_x is the local Nusselt number

$$Nu_x = \frac{qx}{k(T_w - T_{\infty})}. \quad (28)$$

(c) Applications

Out of the multitude of wall temperatures represented by expression (5), the two most important ones seem to be: (1) the constant wall temperature; (2) the one giving rise to a constant wall heat flux. The first case has already been dealt with as a separate problem by Sparrow and Gregg [6]. On taking $m = 0$ and $a_n = 0$, the present analysis naturally completely coincides with the one of these authors. The second problem is still open for thorough investigation. As far as the author is aware of, no results of experimental work concerning this matter have been published. Yet the set-up of an experiment seems to be most simple in the case of the constant wall heat flux. One merely has to lead an electric current through a vertical metallic constant-property wire, suspended in some gas or liquid. For comparison with future experiments, it therefore seems reasonable to supply a large body of theoretical results here.

Constant wall-heat flux. Though not totally in conformity with the set-up of the present investigations, where the surface-temperature is a given quantity, the problem of constant wall-heat flux quite well falls within the scope of these investigations, as will be shown below. At the root of this problem is the condition that q in equation (25) be constant. From (20) and (26) now easily can be derived ($m = 0.2$)

$$q = -k \left(\frac{g\beta N^5}{4\nu^2 l} \right)^{\frac{1}{4}} \sum_{n=0}^{\infty} \theta'_n(0) \xi^n. \quad (29)$$

Hence

$$\theta'_n(0) = 0 \quad \text{for } n > 0, \quad (30)$$

$$q = -k \left(\frac{g\beta N^5}{4\nu^2 l} \right)^{\frac{1}{4}} \theta'_0(0). \quad (31)$$

Here it has to be mentioned that on account of the fact that the wall temperature is unknown, the constant N is also unknown. Solution of N from (31) and substitution in (15) gives the wall temperature induced on a cylinder by a constant heat flux q

$$T_w = T_\infty + \left(\frac{4v^2 q^4 x}{g\beta k^4} \right)^{\frac{1}{4}} \{-\theta'_0(0)\}^{-\frac{1}{4}} \sum_{n=0}^{\infty} \theta_n(0) \xi^n. \quad (32)$$

It can easily be proved that the system of equations (24) is invariant under the transformation

$$f_0(\eta) = \gamma f_0(\gamma\eta); \quad \theta_0(\eta) = \gamma^4 \bar{\theta}_0(\gamma\eta). \quad (33)$$

From (33) then follows by differentiation with respect to η , elimination of γ and for σ given

$$\{-\theta'_0(0)\}^{-\frac{1}{4}} \theta_0(0) = \{-\bar{\theta}'_0(0)\}^{-\frac{1}{4}} \bar{\theta}_0(0). \quad (34)$$

Consequently the constant (34) occurring in equation (32) can be calculated by imposing whatever boundary condition on θ_0 at $\eta = 0$. Here this condition has been chosen to be $\theta_0(0) = 1$. For θ_n ($n > 0$) the boundary conditions at $\eta = 0$ are naturally embodied in equation (30). The problem now is nearly completely in accordance with the original set-up, the difference lying in the fact that the constants a_n or h , instead of being known from the start, have to be determined in such a way as to ensure that $\theta'_n(0) = 0$ ($n > 0$). In Table 1 the

Table 1

σ	$4^{\frac{1}{4}}\{-\theta'_0(0)\}^{-\frac{1}{4}}$	$\theta_0(0)$	$\theta_1(0)$	$\theta_2(0)$
0.7	2.068533	-0.570081	-0.29424	0.1063
1	1.872838	-0.645490	-0.26064	0.0830
2	1.559112	-0.811743	-0.20879	0.0529
3	1.408018	-0.922050	-0.18467	0.0413
4	1.312465	-1.006712	-0.16969	0.0348
5	1.244133	-1.076295	-0.15910	0.0306
7	1.149541	-1.188117	-0.14461	0.0253
10	1.059004	-1.316415	-0.13096	0.0203

results of a numerical integration have been given for a variety of Prandtl numbers covering ordinary liquids and gases. Of foremost interest is the fact that for all Prandtl numbers the first perturbation has negative sign, showing that the temperature induced on a cylinder increases less rapidly with x than that induced on a flat plate. Here it has to be remembered that the equivalent

flat plate problem is depicted by the first term of the series.

Obviously this effect has to be explained by considering that a cylinder is in much closer contact with its environments (all-sided contact) than a flat plate is.

It is interesting to investigate whether radial curvature effects are decreased by variation of the various parameters of the system. To that end one may consider the ratio of the first and zeroth perturbation of $T_w - T_\infty$ (32).

On deriving the correct representation of ξ for the present case, one finds for this ratio:

$$\theta_1(0) \xi = \frac{2\theta_1(0)}{r_0} \left(\frac{-4v^2 \theta'_0(0) kx}{g\beta q} \right)^{\frac{1}{4}}. \quad (35)$$

The conclusions to be given naturally are based upon the consideration that a larger value of equation (35) is equivalent with a greater influence of radial curvature.

The way in which the influence of radial curvature is affected by the different parameters of the system, can be investigated best by varying one of these parameters and leaving the others constant. It is easily seen then from equation (35) that through increasing r_0 , g , β or q or through decreasing x the radial curvature is losing influence. For ρ , c_p the investigation is somewhat more complicated since these quantities appear implicitly in equation (35) through σ and thus through $\theta_1(0)\{-\theta'_0(0)\}^{\frac{1}{4}}$. v and k appear both implicitly and explicitly in (35). Upon writing

$$v^{\frac{1}{4}} \theta_1(0) \{-\theta'_0(0)\}^{\frac{1}{4}} = \left(\frac{k}{\rho c_p} \right)^{\frac{1}{4}} \theta_1(0) \{-\sigma^2 \theta'_0(0)\}^{\frac{1}{4}} \quad (36)$$

and

$$\theta_1(0) \{-k\theta'_0(0)\}^{\frac{1}{4}} = (v\rho c_p)^{\frac{1}{4}} \theta_1(0) \left\{ -\frac{\theta'_0(0)}{\sigma} \right\}^{\frac{1}{4}} \quad (37)$$

it is understood that the effect of v and k can be studied through variation of σ . Table 2 shows

Table 2

σ	$\theta_1(0) \{-\theta'_0(0)\}^{\frac{1}{2}}$	$\theta_1(0) \{-\sigma^2 \theta'_0(0)\}^{\frac{1}{2}}$	$\theta_1(0) \left\{ -\frac{\theta'_0(0)}{\sigma} \right\}^{\frac{1}{2}}$
0.7	-0.262955	-0.227993	-0.282398
1	-0.238791	-0.238791	-0.238791
2	-0.200259	-0.264243	-0.174336
3	-0.181699	-0.281968	-0.145857
4	-0.169914	-0.295838	-0.128771
5	-0.161457	-0.307358	-0.117021
7	-0.149684	-0.325998	-0.101428
10	-0.138359	-0.347542	-0.087299

that increasing ρ or c_p or decreasing k or v diminishes the influence of radial curvature.

Numerical values of the dimensionless group (27) can be calculated with the figures given in Table 1.

In addition to the results of Table 1 concerning heat transfer, it seems worthwhile to plot temperature and velocity profiles. Graphs of f'_0 , f'_1 , f'_2 , θ_0 , θ_1 and θ_2 are presented in Figs. 2 and 3. Here the Prandtl number σ has been taken equal to 0.7 (air). The functions f'_i naturally are related to the longitudinal velocity u which can be shown directly through substitution of (8) and (14) in equation (4). It is interesting to study the influence of the higher perturbations on the velocity and temperature

profiles. To that end $\partial f / \partial \eta$ and θ are shown in the Figs. 4 and 5 for $\xi = 0$ and $\xi = 0.2$. If attention is given first to the velocity profiles (Fig. 4), it is seen that the maximum velocity decreases as ξ increases. This result has to be expected on account of the fact that smaller temperature differences give rise to smaller velocities. For both the velocity and the temperature layer, it is seen that these layers flatten out less rapidly as ξ becomes larger.

It should be remarked that the same qualitative features are exhibited for the other values of the Prandtl number considered in this paper.

3. CONE

In case ϕ has a constant positive value less than $\pi/2$ the equations (1), (2) and (3) govern free convection along a vertical cone. In view of the assumption about the temperature excess at the wall, the vertex of the cone ($x = 0$), will be pointed in downward direction (Fig. 6). In a number of papers [10-13] free convection past a cone has been studied already. Most extensively this has been done by Hering and Grosh [13], who considered wall temperatures as given in equation (5) with $h = 1$. These papers, however, are based upon a momentum and energy equation which do not involve curvature terms. Cones for which ϕ is not small—the

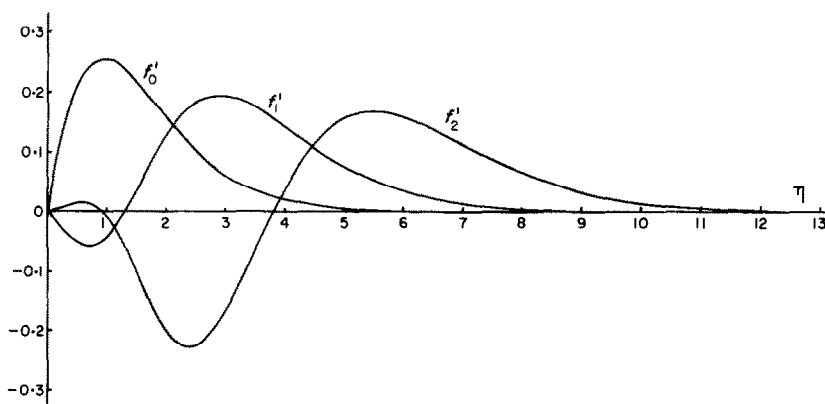


FIG. 2. Perturbations of the velocity-distribution for cylinder at uniform wall heat flux ($\sigma = 0.7$).

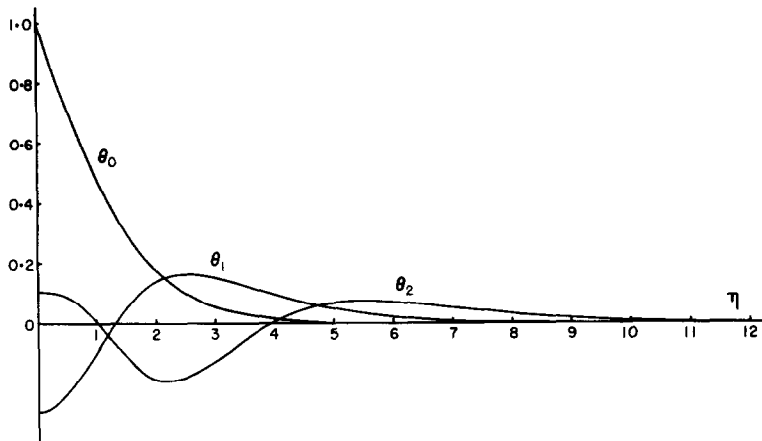


FIG. 3. Perturbations of the temperature-distribution for cylinder at uniform wall heat flux ($\sigma = 0.7$).

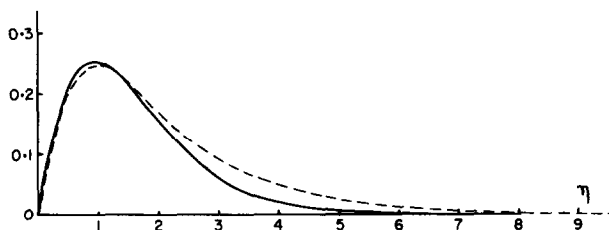


FIG. 4. Velocity profiles for $\xi = 0$ (solid) and $\xi = 0.2$ (dotted) for cylinder at uniform wall heat flux ($\sigma = 0.7$).

exact determination of what actually is “small” should follow from the present analysis—the neglect of these terms does not seriously affect solution, apart from a small region near the vertex of the cone. However, the equations used here and in the papers just mentioned, can only be applied to slender cones, because of the fact that no buoyancy effect in the y -direction is taken into account. For slender cones it may be expected that the region of large transverse curvature is extended. Using the full equations (2) and (3) it will be endeavoured, through applying a perturbation technique analogous to that used for the cylinder, to find a solution valid in a larger region than those discounting curvature.

(a) Solution

Using the same arguments as were given for the cylinder, the successive introduction of

$$\xi = \frac{2}{c_1 \tan \phi} \bar{x}^{-\frac{m+3}{4}}, \quad (38)$$

$$\eta = \frac{(y + x \tan \phi)^2 - x^2 \tan^2 \phi}{\xi x^2 \tan^2 \phi}, \quad (39)$$

$$\psi = \nu l c_1 \tan \phi \bar{x}^{\frac{m+7}{4}} f(\xi, \eta), \quad (40)$$

with

$$c_1 = \left(\frac{g \beta N l^3 \cos \phi}{\nu^2} \right)^{\frac{1}{4}} \quad (41)$$

can be proved to be justified.

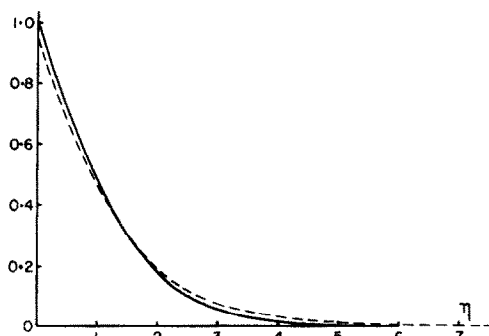


FIG. 5. Temperature profiles for $\xi = 0$ (solid) and $\xi = 0.2$ (dotted) for cylinder at uniform wall-heat flux ($\sigma = 0.7$).

Anticipating already that ξ is destined to be an expansion variable the role of ϕ becomes clear. It turns out that ξ grows as ϕ decreases. On considering free convection of a gas ($\nu \sim 10^{-5}$, $\beta \sim \frac{1}{300}$) past a cone (with $\phi = 5^\circ$) having a surface-temperature exceeding that of the ambient gas by 30 degK, it follows that for $x = 1$ ξ is $O(0.1)$. Hence the transverse curvature effects are strong for a part of the cone which is as long as 1 m!

On insertion of the equations (4, 15, 38–41) in (2) and (3), the non-dimensional momentum-energy equations are found to be

$$\frac{\partial^3 f}{\partial \eta^3} + \frac{m+7}{4} f \frac{\partial^2 f}{\partial \eta^2} - \frac{m+1}{2} \left(\frac{\partial f}{\partial \eta} \right)^2 + \theta + \xi \left[\eta \frac{\partial^3 f}{\partial \eta^3} + \frac{\partial^2 f}{\partial \eta^2} + \frac{m+3}{4} \left(\frac{\partial f}{\partial \eta} \frac{\partial^2 f}{\partial \eta \partial \xi} - \frac{\partial f}{\partial \xi} \frac{\partial^2 f}{\partial \eta^2} \right) \right] = 0, \quad (42)$$

$$\frac{1}{\sigma} \frac{\partial^2 \theta}{\partial \eta^2} + \frac{m+7}{4} f \frac{\partial \theta}{\partial \eta} - m \theta \frac{\partial f}{\partial \eta} + \xi \left[\frac{1}{\sigma} \left(\frac{\partial \theta}{\partial \eta} + \eta \frac{\partial^2 \theta}{\partial \eta^2} \right) + \frac{m+3}{4} \left(\frac{\partial f}{\partial \eta} \frac{\partial \theta}{\partial \xi} - \frac{\partial f}{\partial \xi} \frac{\partial \theta}{\partial \eta} \right) \right] = 0. \quad (43)$$

Substitution of the expansions (19) and (20) in the equations (42) and (43) renders again an

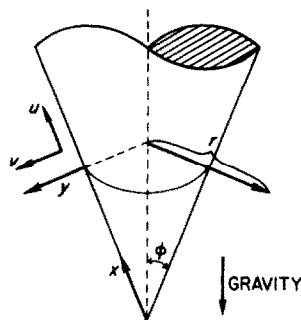


FIG. 6. Geometrical configuration for flow past cone.

infinite set of ordinary differential equations, having the same features as those found for the cylinder. The first set of two differential equations is the same as that of Hering and Grosh. It is worthy noting that for $m > -3$, the expansion variable ξ vanishes as $x \rightarrow \infty$. This is in conformity with the vanishing of the influence of radial curvature in that direction and the increasing of it on approaching the vertex.

(b) Heat transfer and results

Using the definitions (25) and (28) for the heat transfer and the Nusselt number, it is easy to derive the non-dimensional group

$$\frac{Nu_x}{Gr_x^{\frac{1}{4}}} = -h^{-\frac{1}{4}} \sum_{n=0}^{\infty} \theta'_n(0) \xi^n. \quad (44)$$

Gr_x is defined as being the expression of (22) multiplied with $\cos \phi$.

The analysis can be illustrated by comparing its results with those of Hering and Grosh. For the cone at constant temperature $T_\infty + N$ ($m = 0$, $h = 1$), the equations have been integrated for $\sigma = 0.7$ and $\sigma = 1$ in order to have an idea of the influence of the Prandtl number (Table 3).

Table 3

σ	$\theta'_0(0)$	$\theta'_1(0)$	$\theta'_2(0)$
0.7	-0.451095	-0.20605	-0.0028
1	-0.510400	-0.20547	-0.0010

Substitution of the figures of Table 3 in equation (44) shows that the first perturbation augments the heat transfer.

An investigation of an expression like (35) will lead to the same conclusions about the effect of the different fluid properties upon the

influence of radial curvature as were presented for the cylinder. Finally, graphs of velocity and temperature profiles are presented in the Figs. 7 and 8. In many respects, these graphs look similar to those given for the cylinder with uniform heat flux through the wall. A notable

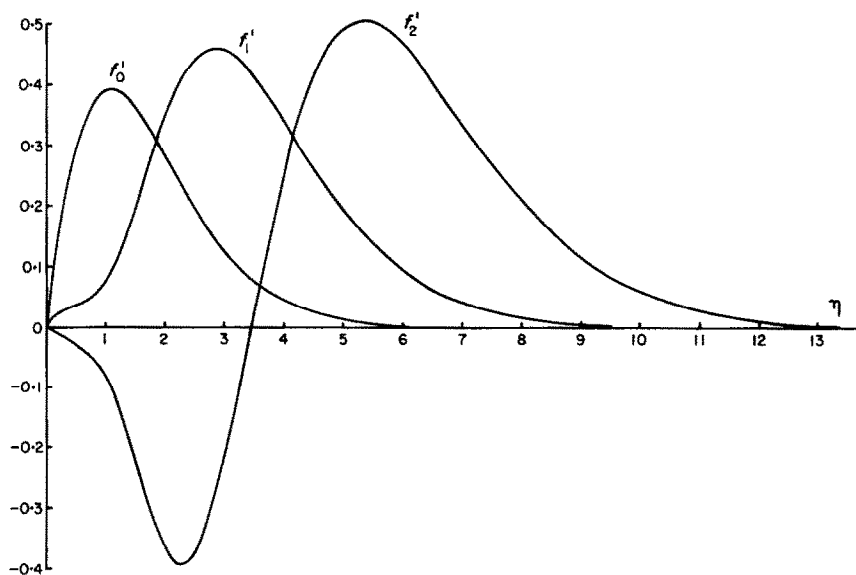


FIG. 7. Perturbations of the velocity-distribution for cone at constant wall-temperature ($\sigma = 0.7$).

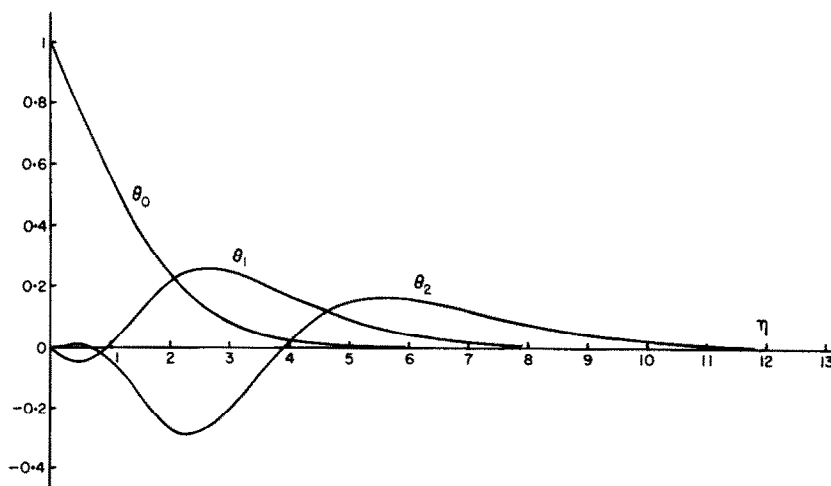


FIG. 8. Perturbations of the temperature-distribution for cone at constant wall-temperature ($\sigma = 0.7$).

difference however is, that the first perturbation of the velocity is not negative near $\eta = 0$, as is the case with the cylinder. This fact is explained in the concluding remarks.

4. CONCLUDING REMARKS

As to the possible values of the parameter m occurring in the temperature distribution (5) the following remark may be made. Numerical calculations of Sparrow and Gregg concerning free convection past a vertical plate under non-uniform wall temperature conditions [14] show that the set of equations (19) can be solved for negative values of m . The range can be extended up to about $m = -1$. For the zero order equations of the cone, no information about this is available, but it is anticipated that here an analogous limit holds. Arguments for this may be found in the well-known linear time-space dependent heat-conduction problem (heat conduction in a rod). If, as a boundary condition, it is imposed that T at some place varies proportionally with t^m (t is the time) then m has to be greater than -1 . The heat source must be of limited strength.

The calculations of this paper have demonstrated unambiguously that an increasing radial curvature yields higher heat-transfer numbers. For the cone at constant temperature, this was directly evident. For the cylinder at constant heat flux it became apparent through considering that a lower temperature was induced on a cylinder than on a flat plate, by the same heat flux. In papers considering forced flows along slender bodies of revolution it has been shown that the radial curvature tends to increase the skin friction [1-5]. It is well-known, and it can be derived easily for the present case, that the skin friction is proportional to $f''(\xi, 0)$. The figures of Table 4 applying to the cone exhibit clearly the behaviour of the skin friction just mentioned. The figures of the cylinder, however, seem to contradict it. Here the following explanation has to be given. In free convection the dynamic part of the problem is completely dependent on the temperature difference with

Table 4

σ	$f_0''(0)$	$f_1''(0)$	$f_2''(0)$
cylinder at constant heat flux			
0.7	0.642010	-0.08439	0.0316
1	0.607040	-0.06758	0.0231
2	0.539515	-0.04449	0.0130
3	0.501085	-0.03507	0.0094
4	0.474541	-0.02970	0.0075
5	0.454433	-0.02613	0.0063
7	0.424990	-0.02158	0.0048
10	0.395030	-0.01766	0.0038
cone at constant temperature			
0.7	0.819590	0.19314	-0.0509
1	0.769427	0.16386	-0.0374

T_∞ inasmuch as the driving force is proportional with this difference. For the problem of the cylinder at constant heat flux, it was seen that the radial curvature diminishes the surface temperature and thus, in a proportional way, the driving force. Obviously there are two tendencies concerning the skin friction counter-acting each other in the problem of constant heat flux. The figures of Table 4 show that the effect in connection with the lower temperature is stronger.

ACKNOWLEDGEMENT

The author is indebted to Mr. P. Veenman, of the Nuclear Division of the Department (Technological University Delft), for pointing out a more accurate method of solving the equations of the higher perturbations than the author used originally.

REFERENCES

1. R. A. SEBAN and R. BOND, Skin friction and heat-transfer characteristics of a laminar boundary layer on a cylinder in axial incompressible flow, *J. Aeronaut. Sci.* **18**, 671-675 (1951).
2. R. M. MARK, Laminar boundary layers on slender bodies of revolution in axial flow, Guggenheim Aeronautical Laboratories, Calif. Inst. Techn. Memo 21 (1954).
3. R. F. PROBSTEIN and D. ELLIOT, The transverse curvature effect in compressible axially symmetric laminar boundary-layer flow, *J. Aeronaut. Sci.* **23**, 208-224 (1956).
4. M. YASUHARA, Axisymmetric viscous flow past very slender bodies of revolution, *J. Aerospace Sci.* **29**, 667-688 (1962).

5. M. H. WEI, Asymptotic boundary layer over a slender body of revolution in axial compressible flow, *AIAA JI* **3**, 809–816 (1965).
6. E. M. SPARROW and J. L. GREGG, The laminar free convection heat transfer from the outer surface of a vertical cylinder, *Trans. Am. Soc. Mech. Engrs* **78**, 1823–1828 (1956).
7. F. R. HAMA and J. CHRISTIAENS, Experiment on the axisymmetric free convection field along a vertically suspended wire, University of Maryland, Institute for Fluid Dynamics TN-BN-138 (1958).
8. K. MILLSAPS and K. POHLHAUSEN, The laminar free convective heat transfer from the outer surface of a vertical circular cylinder, *J. Aeronaut. Sci.* **25**, 357–360 (1958).
9. K-T. YANG, Possible similarity solutions for laminar free convection on vertical plates and cylinders, *J. Appl. Mech.* **26**, 230–236 (1960).
10. H. J. MERK and J. A. PRINS, Thermal convection in laminar boundary layers I, *Appl. Scient. Res.* **A4**, 11–24 (1953).
11. W. H. BRAUN and J. E. HEIGHWAY, An integral method for natural convection flows at high and low Prandtl numbers, N.A.S.A., TN D-292 (1960).
12. W. H. BRAUN, S. OSTRACH and J. E. HEIGHWAY, Free convection similarity flows about two dimensional and axisymmetric bodies with closed lower ends, *Int. J. Heat Mass Transfer* **2**, 121–135 (1961).
13. R. G. HERING and R. J. GROSH, Laminar free convection from a non-isothermal cone, *Int. J. Heat Mass Transfer* **5**, 1059–1068 (1962).
14. E. M. SPARROW and J. L. GREGG, Similar solutions for free convection from a non-isothermal vertical plate, *Trans. Am. Soc. Mech. Engrs* **80**, 379–386 (1958).
15. M. FINSTON, Free convection past a vertical plate, *Z. Angew. Math. Phys.* **7**, 527–529 (1956).
16. S. OSTRACH, in *Theory of Laminar Flows*, edited by F. K. MOORE, pp. 528–712. Princeton University Press, Princeton (1964).
17. H. GÖRTLER, A new series for the calculation of steady laminar boundary layer flows, *J. Math. Mech.* **6**, 1–66 (1957).

Résumé—Les effets de courbure radiale sur la couche limite de convection naturelle avec symétrie de révolution sont étudiés pour des cylindres verticaux et des cônes dans le cas de certaines différences de température non uniforme entre la surface et le fluide ambiant. On donne la solution sous forme d'un développement en série de puissances, le premier terme étant égal à la solution qu'on trouve lorsqu'on ne fait pas intervenir de courbure transversale. Des intégrations numériques ont été effectuées pour différents nombres de Prandtl. Une application intéressante est la détermination de la température de la surface d'un cylindre refroidi par convection naturelle avec flux de chaleur constant à travers la surface. Pour les nombres de Prandtl considérés, il se trouve que le même flux de chaleur produit une température pariétale plus faible sur un cylindre que sur une plaque.

Zusammenfassung—Einflüsse radialer Krümmung auf achssymmetrische Grenzschichtströmungen auf Grund freier Konvektion werden an senkrechten Zylindern und Kegeln untersucht für spezielle nicht-einheitliche Temperaturdifferenzen zwischen Oberfläche und umgebendem Medium. Die Lösung ist in Form einer Potenzreihe angegeben, wobei der erste Ausdruck gleich ist dem der Lösung für den Fall, dass keine Krümmung in Querrichtung vorliegt. Für eine Reihe von Prandtl-Zahlen wurden numerische Integrationen durchgeführt. Eine interessante Anwendung stellt die Bestimmung der Oberflächentemperatur eines durch freie Konvektion gekühlten Zylinders dar bei konstantem Wärmestrom durch die Oberfläche. Es zeigt sich, dass im Bereich der untersuchten Prandtl-Zahlen bei gleichem Wärmestrom, am Zylinder eine geringere Oberflächentemperatur auftritt als an einer ebenen Platte.

Аннотация—Исследуется влияние радиальной кривизны на осесимметричный пограничный слой при свободной конвекции при обтекании вертикальных цилиндров и конусов для некоторых частных случаев неравномерной разности температур поверхности и окружающей среды. Решение дается в виде степенного ряда, первый член которого является решением для случая отсутствия поперечной кривизны. Проведено численное интегрирование для ряда чисел Прандтля. Интересным практическим случаем является определение поверхностной температуры цилиндра, охлаждаемого свободной конвекцией при постоянном тепловом потоке через поверхность. Оказалось, что для рассматриваемых чисел Прандтля при одинаковой величине теплового потока температура поверхности цилиндра ниже, чем на плоской пластине.